SkyPole-A method for locating the north celestial pole from skylight polarization patterns

Thomas Kronland-Martinet, Léo Poughon, Marcel Pasquinelli, David Duché, Julien R Serres, Stéphane Viollet

PNAS BRIEF REPORT | ENGINEERING ECOLOGY OPEN ACCESS

SkyPole—A method for locating the north celestial pole from skylight polarization patterns

Thomas Kronland-Martinet[a,b], Léo Poughon[a], Marcel Pasquinelli[b], David Duché[b], Julien R. Serres[a,c], and Stéphane Viollet[a,1]

Edited by Hui Cao, Yale University, New Haven, CT; received March 24, 2023; accepted June 10, 2023

True north can be determined on Earth by three means: magnetic compasses, stars, and via the global navigation satellite systems (GNSS), each of which has its own drawbacks. GNSS are sensitive to jamming and spoofing, magnetic compasses are vulnerable to magnetic interferences, and the stars can be used only at night with a clear sky. As an alternative to these methods, nature-inspired navigational cues are of particular interest. Celestial polarization, which is used by insects such as *Cataglyphis* ants, can provide useful directional cues. Migrating birds calibrate their magnetic compasses by observing the celestial rotation at night. By combining these cues, we have developed a bioinspired optical method for finding the celestial pole during the daytime. This method, which we have named SkyPole, is based on the rotation of the skylight polarization pattern. A polarimetric camera was used to measure the degree of skylight polarization rotating with the Sun. Image difference processes were then applied to the time-varying measurements in order to determine the north celestial pole's position and thus the observer's latitude and bearing with respect to the true north.

celestial navigation | celestial compass | polarized vision | geolocation | GPS-denied environment

During the last few decades, many high-precision geolocation tools have emerged thanks to Global Navigation Satellite Systems (GNSS) (1). However, GNSS-based position estimates are sometimes unreliable because of the multipath reception involved (2) and their sensitivity to jamming and spoofing. To overcome this problem, inertial navigation systems (INS) have been used to obtain position and orientation by implementing dead reckoning methods (3). However, INS suffer from a loss of precision in time due to the accumulating sensor measurement errors. Navigation issues have also been successfully handled by some animals by processing scarce information using simple navigational methods. The authors of neuro-ethological studies have described the use of skylight polarization patterns by insects such as desert ants for navigation purposes (4). Several studies have also established that migratory birds, such as Indigo Buntings (5, 6) and Savannah Sparrows (7), calibrate their magnetic compass at night by observing the dynamic movements of stars around the celestial pole (8). On similar lines, migratory songbirds calibrate their magnetic compass during the daytime on the basis of skylight polarization patterns (9, 10). Skylight polarization can be described by Rayleigh's single scattering model (11), in which sunlight is assumed to be scattered by small particles present in the Earth's atmosphere. Based on this model, cheap and reliable GPS-free polarization-based navigation methods have been developed. For instance, by mimicking the *Cataglyphis* desert ant, a polarization-based optical compass can provide a reference local bearing defined with respect to the polarization pattern in the sky (12, 13). However, like ordinary INS, polarization-based INS also suffers from integration drift. To overcome this problem, direct geopositioning can be achieved based on skylight polarization patterns without any need for GPS. By estimating the Sun's position from the skylight polarization pattern and combining this information with complex calculations (solar ephemeris), the observer's position can be computed (14–16). However, animals do not have access to ephemeris, and their use of polarization as a local or global reference for navigation purposes has not yet been completely elucidated.

In line with previous assumptions about the perception of polarized light by animals, we have adopted the suggestion put forward by Brines (17) that the temporal properties of the skylight polarization pattern can be regarded as a strong useful navigation cue. We developed a bioinspired method to find the geographical north bearing and the observer's latitude, requiring only skylight polarization observations.

Skylight is mostly linearly polarized and characterized by two parameters: the angle of linear polarization (AoLP) and the degree of linear polarization (DoLP). The present method consists in comparing skylight DoLP images taken at different moments, in

Author affiliations: [a]Aix Marseille University, CNRS, ISM, Marseille 13009, France; [b]Aix Marseille University, CNRS, IM2NP, Marseille 13013, France; and [c]Institut Universitaire de France, Paris 75005, France

Author contributions: T.K.-M., J.R.S. and S.V. designed research; T.K.-M. and L.P. performed research; T.K.-M., L.P., M.P., D.D., J.R.S., and S.V. analyzed data; and T.K.-M., J.R.S., and S.V. wrote the paper.

The authors declare no competing interest.

[1]To whom correspondence may be addressed. Email: stephane.viollet@univ-amu.fr.

This article contains supporting information online at https://www.pnas.org/lookup/suppl/doi:10.1073/pnas.2304847120/-/DCSupplemental.

Published July 17, 2023.

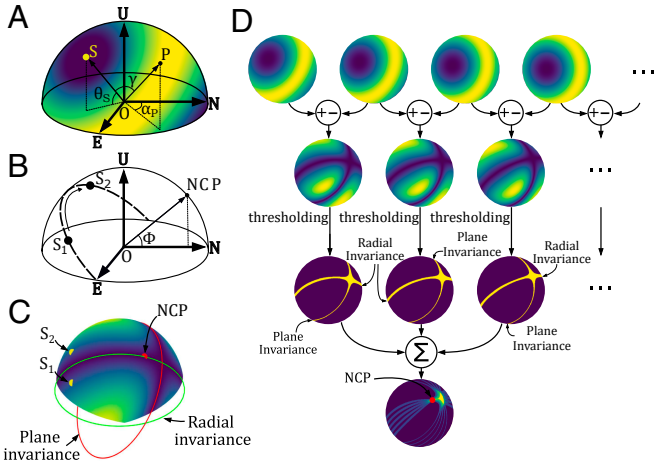

Fig. 1. (*A*) Scattering angle γ, azimuth α_P of a point P, and altitude θ_S of the Sun S. Parameters are presented in the ENU frame, namely East, North, and Up frame, centered on the observer O. The colored patterns stand for the skylight DoLP as described in Eq. **1**. Dark blue corresponds to near-zero DoLP and yellow to maximum DoLP values (1 in theory, less in reality). (*B*) The trajectory of the Sun in the ENU frame, centered on an observer O located at latitude ϕ. NCP is the north celestial pole. The Sun moves on a plane perpendicular to the observer–NCP vector. (*C*) Invariance axis on the celestial sphere. Comparison between simulated and analytical sets of solutions. The green circle is the radial invariance circle; the red circle is the plane invariance circle computed from analytical calculations (cf. *SI Appendix*). The colored half sphere is the simulated absolute difference between two DoLP patterns associated with the Sun's positions S_1 and S_2 at two different times. Dark blue corresponds to near-zero values. The red dot is the NCP. (*D*) Method for finding the NCP based on the skylight's DoLP pattern. In the first row are the DoLP patterns taken at four different times. Absolute differences between DoLP patterns were then computed, giving the second row. A thresholding step was then applied to those images, and the results are presented in the third row. Last, binary images were summed, and the NCP was then located at the intersection between the radial invariances.

order to find the north celestial pole (NCP). The geographical north bearing and the observer's latitude can then be deduced from the NCP coordinates.

Numerical Simulations of the SkyPole Method

When sun rays enter the atmosphere, Rayleigh scattering occurs, resulting in an observable pattern of skylight polarization depending on the Sun's position. As described by the single scattering Rayleigh model, skylight polarization is mostly linear, and two quantities describing this phenomenon can therefore be observed, namely the direction of linear polarization and the DoLP. In this study, we focused on the DoLP, which is defined by the ratio between the polarized light intensity and the total light intensity. In the Rayleigh single scattering model, the pattern of DoLP can be described as follows (11):

$$DoLP(\gamma) = \frac{1 - \cos^2(\gamma)}{1 + \cos^2(\gamma)}, \qquad [1]$$

where γ is the scattering angle (cf. Fig. 1*A*).

Eq. **1** describes two noteworthy properties of the DoLP pattern: its radial symmetry about the solar vector and the plane symmetry about the plane perpendicular to the solar vector, including the reference point O (Fig. 1*A*). Therefore, as depicted in Fig. 1*C*, when the Sun has shifted from an initial position, the resulting shifted DoLP pattern remains unchanged on two axes due to the symmetry of the DoLP function. From now on, we will refer to these invariances as radial and plane invariance. Similar patterns in the magnetic field might be seen by migratory birds to find north (18). We computed the difference between the images of the two patterns of DoLP taken at two distinct moments (with time intervals ranging from 30 to 60 minutes) in order to display the radial and plane invariance axes (Fig. 1*C*). Since the Sun rotates around the NCP (the south celestial pole as perceived by an observer in the Southern hemisphere, cf. ref. 19 for further details), the scattering angle γ is constant at this point, and therefore, the DoLP at the NCP will remain constant at all times of day. The NCP is located on the radial invariance circle, and this is the only visible point on the celestial sphere which is present at all times on this axis (cf. *SI Appendix*). The NCP can therefore be found at the intersection between the radial invariance axes resulting from time-varying DoLP image differences. Theoretically, only three views of the sky's DoLP pattern are necessary for computing the position of the NCP.

Results

The SkyPole algorithm was tested on data recorded with a polarimetric camera equipped with a fisheye lens. The camera was placed on the roof of a laboratory in Marseille, France (43.286987°N, 5.4032786°E) giving a quasi-hemispherical view of the sky dome. The SkyPole algorithm described in Fig. 1*D* was applied to DoLP images of the sky in order to locate the NCP and assess the accuracy of the method. As the NCP is located in the sky at an azimuth equal to that of the geographical north and an altitude equal to the observer's latitude, the latitude and north bearing measured were compared with the ground truth values obtained from the solar ephemeris. As shown in Fig. 2, the results obtained by applying the SkyPole method to experimental data (20) were consistent with the simulated results presented in Fig. 1*D*. We also estimated the NCP's position with an azimuth of the camera ranging from 0 to 170° in steps of 10° (cf. Fig. 3). A mean absolute azimuth error of 2.6° and a mean absolute latitude error of 3.8° were obtained.

Discussion

The method presented here for locating the NCP requires only visual observations of the skylight polarization patterns. No

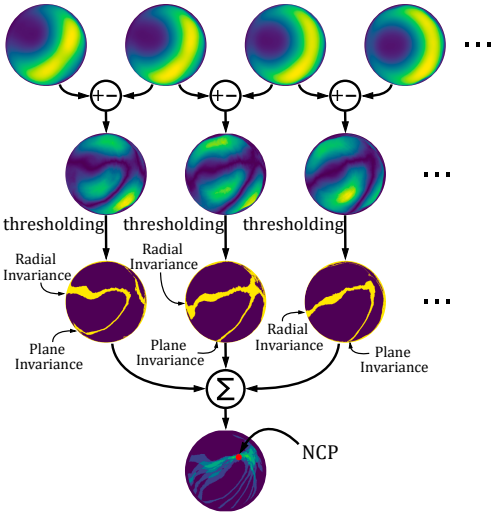

Fig. 2. SkyPole algorithm applied to experimental data for finding the NCP. Preprocessing of the first row of DoLP images consisted in filtering the images obtained using a circular averaging filter. Details of the following steps are presented in Fig. 1*D*.

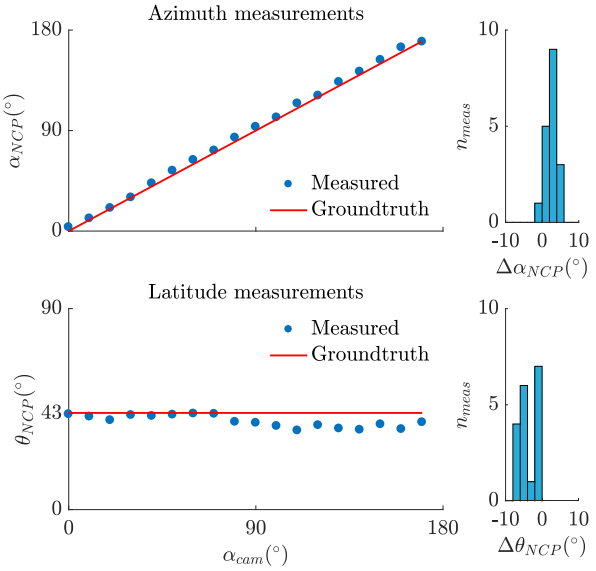

Fig. 3. NCP coordinates computed with the SkyPole algorithm (Fig. 2) from experimental data versus ground truth NCP coordinates. α_{cam} is the azimuth of the camera with respect to the north. α_{NCP} is the azimuth of the NCP with respect to the azimuth of the camera. θ_{NCP} is the altitude of the NCP, which is also equal to the camera's latitude. $\Delta\alpha_{NCP}$ and $\Delta\theta_{NCP}$ are the azimuth and altitude error, respectively, of the NCP measured with respect to the ground truth values. n_{meas} is the number of measurements for each error interval.

knowledge of time, date, or ephemeris, and no estimates of the actual or initial position are required for this purpose. The image-processing steps do not rely on large computational resources. The efficiency of our method has been proved in simulations and under experimental conditions, thus confirming the validity of the theoretical model (cf. *SI Appendix*).

The accuracy of our algorithm may also seem rather too low for some geolocation applications. It is worth noting, however, that this algorithm has been kept as simple as possible, and that more sophisticated data processing algorithm would no doubt greatly improve the accuracy. Most of the errors in the NCP position estimates can be explained by two different sources of noise: skylight noise and camera noise. Skylight noise originates from multiple scattering or non-Rayleigh scattering in the atmosphere, such as Mie scattering, for instance. In this study, in order to reduce the influence of this kind of noise, we used data with low noise levels, corresponding to a clear blue sky or an only slightly overcast sky. In future studies, special emphasis should be placed on image filtering in order to reduce the influence of noise. In addition, in the case of both simulated and measured observations, each NCP position estimation process required several hours of observation. In this study, the aim was to find the NCP using only the radial invariance of the difference between skylight DoLP patterns. However, the point visible at the intersection between plane invariance and radial invariance gives the sky's maximum DoLP value, which gives direct information about the Sun's elevation.

Materials and Methods

The SkyPole method was tested with data collected from a Rayleigh sky simulation. We also tested our method with experimental data obtained with a calibrated Lucid Vision Lab PHX050S-QC, division of focal plane polarimetric camera. Our data were first preprocessed with a circular averaging filter. Next, we implemented the absolute difference in DoLP between several moments of time. We then applied a threshold-based binarization algorithm. Next, in order to obtain the NCP, several binary images were added. The NCP was located by searching for the maximum valued point, namely the intersection between all the radial invariance axes (cf. Fig. 1*D*). Last, the coordinates of the point were transformed to north and latitude coordinates and compared with the ground truth values. Additional experiments and data are available here: https://osf.io/fcsgk/.

Conclusion

In this paper, a method is presented for finding the NCP in the daytime by measuring the skylight polarization patterns. This method gives an estimate of the bearing toward the Geographical North Pole and the latitude of the observer.

Our minimalistic SkyPole algorithm could suggest a hypothesis in terms of possible visual processing steps used by animals to navigate. With a relatively long acquisition time, SkyPole may not be sufficient for autonomous navigation. However, SkyPole might be implemented on board future geolocation systems to provide navigation information in GPS-denied environments since it requires only skylight polarization observations.

Data, Materials, and Software Availability. Code and data images have been deposited in Open Science Foundation.

1. B. Renfro, M. Stein, E. Reed, J. Morales, E. Villalba, *An Analysis of Global Positioning System (GPS) Standard Positioning Service Performance for 2019* (University of Texas, Austin, 2020), pp. 1–111.
2. T. Kos, I. Markezic, J. Pokrajcic, "Effects of multipath reception on GPS positioning performance" in *Proceedings ELMAR-2010* (2010), pp. 399–402.
3. Y. Alkendi, L. Seneviratne, Y. Zweiri, State of the art in vision-based localization techniques for autonomous navigation systems. *IEEE Access* **9**, 76847–76874 (2021).
4. R. Wehner, *Desert Navigator: The Journey of an Ant* (Harvard University Press, 2020).
5. S. Emlen, The ontogenetic development of orientation capabilities. *NASA Spec. Publ.* **262**, 191 (1972).
6. S. T. Emlen, Celestial rotation: Its importance in the development of migratory orientation. *Science (New York, N.Y.)* **170**, 1198–1201 (1971).
7. K. Able, M. Able, Calibration of the magnetic compass of a migratory bird by celestial rotation. *Nature* **347**, 378–380 (1990).
8. J. L. Gould, C. G. Gould, "Nature's compass" in *Nature's Compass* (Princeton University Press, 2012).
9. K. Able, M. Able, Manipulations of polarized skylight calibrate magnetic orientation in a migratory bird. *J. Comp. Physiol. A* **177**, 351–356 (1995).
10. W. W. Cochran, H. Mouritsen, M. Wikelski, Migrating songbirds recalibrate their magnetic compass daily from twilight cues. *Science* **304**, 405–408 (2004).
11. K. Coulson, *Polarization and Intensity of Light in the Atmosphere* A. DEEPAK Pub., Hampton, Virginia, USA, (1988).
12. J. Dupeyroux, J. Serres, S. Viollet, AntBot: A six-legged walking robot able to home like desert ants in outdoor environments. *Sci. Robot.* **4**, eaau0307 (2019).
13. E. Gkanias, B. Risse, M. Mangan, B. Webb, From skylight input to behavioural output: A computational model of the insect polarised light compass. *PLoS Comput. Biol.* **15**, e1007123 (2019).
14. Z. Cheng, T. Mei, H. Liang, Positioning algorithm based on skylight polarization navigation. *IFAC Proc. Vol.* **46**, 97–101 (2013).
15. G. Guan, J. Gu, M. Wu, The novel method of North-finding based on the skylight polarization. *J. Eng. Sci. Technol. Rev.* **6**, 107–110 (2013).
16. J. Yang, X. Liu, Q. Zhang, T. Du, L. Guo, Global autonomous positioning in GNSS-challenged environments: A bioinspired strategy by polarization pattern. *IEEE Trans. Ind. Elect.* **68**, 6308–6317 (2020).
17. M. Brines, Dynamic patterns of skylight polarization as clock and compass. *J. Theor. Biol.* **86**, 507–512 (1980).
18. S. Worster, H. Mouritsen, P. Hore, A light-dependent magnetoreception mechanism insensitive to light intensity and polarization. *J. R. Soc. Interface* **14**, 20170405 (2017).
19. W. M. Smart, *Textbook on Spherical Astronomy*, R. M. Green, Ed. (Cambridge University Press, ed. 6, 1977).
20. T. Kronland-Martinet, S. Viollet, SkyPole. Open Science Foundation. https://osf.io/fcsgk/. Deposited 17 May 2023.

Supporting Information for

SkyPole - A method for locating the North Celestial Pole from the skylight polarization patterns

Thomas Kronland-Martinet, Léo Poughon, Marcel Pasquinelli, David Duché, Julien R Serres and Stéphane Viollet

Corresponding author : Stéphane Viollet.
E-mail: stephane.viollet@univ-amu.fr

This PDF file includes:

Supporting Information Text

We provide here a mathematical explanation of the SkyPole method.

For readers unfamiliar with spherical astronomy, we highly recommend the reading of Smart's textbook on spherical astronomy (1). In particular, chapter II, "The Celestial Sphere" provides useful illustrated definitions.
Warning, Symbols used in this document might differ from those used in (1).

Preliminary hypotheses

For the sake of simplicity, we made the following hypotheses:

1. we assume that the rotation of the Earth around the Sun, as well as the movements of nutation and precession of the Earth can be neglected. Therefore, the scattering angle between the Sun and the celestial pole can be considered constant on a short time period of about one day or less;

2. we consider only Rayleigh single scattering, even though Mie scattering and multiple scattering occur in the atmosphere. This hypothesis is yet reasonable as it has been shown that Rayleigh scattering described quite faithfully the skylight polarization (2). We also consider that the maximum value of skylight degree of linear polarization (DoLP) is constant during the observation time. Therefore, this value will not appear in the calculus;

3. we only consider observations made on the Earth north hemisphere. Therefore, only the north celestial pole (NCP) will be evoked. However, the calculations are similar for observations made on the south hemisphere.

Mathematical materials related to DoLP invariances

In this section, we will demonstrate that the DoLP is time invariant at the NCP. We will also introduce the sets of DoLP time invariant points.

If we consider the origin O of the ENU frame, and a point P on the celestial sphere, the vector going from O to P is noted $\overrightarrow{P}$ in all the document. We consider $\overrightarrow{P}$ as a unit vector

Let us define $\overrightarrow{S}$, the Sun vector. The Sun vector with respect to the latitude ϕ, the declination δ and the hour angle ω in the ENU (East, North, Up/Zenith) frame is defined as follows (cf. (3)):

$$\overrightarrow{S} = -\cos\delta\sin\omega\overrightarrow{E} + (\sin\delta\cos\phi - \cos\delta\sin\phi\cos\omega)\overrightarrow{N} + (\cos\delta\cos\phi\cos\omega + \sin\delta\sin\phi)\overrightarrow{Z} \quad [1]$$

Where $\phi \in [-\frac{\pi}{2}, \frac{\pi}{2}]$, $\delta \in [-0.41, 0.41]$, and $\omega = (hour - 12)15°$, with $hour$ the local apparent solar time (0-24h), such as in radians, $\omega \in [-\pi, \pi]$. For the sake of simplicity, we will suppose $\phi \in]-\frac{\pi}{2}, \frac{\pi}{2}[$

Let us consider a point P, whose scattering angle is given by the time dependant function γ_P. The DoLP at the point P is invariant between two times t_1 and t_2 if and only if :

$$\begin{aligned} DoLP(\gamma_P(t_1)) = DoLP(\gamma_P(t_2)) &\iff \frac{1-\cos^2(\gamma_P(t_1))}{1+\cos^2(\gamma_P(t_1))} = \frac{1-\cos^2(\gamma_P(t_2))}{1+\cos^2(\gamma_P(t_2))} \iff \cos^2(\gamma_P(t_1)) = \cos^2(\gamma_P(t_2)) \\ &\iff \cos(\gamma_P(t_1)) = \pm\cos(\gamma_P(t_2)) \iff \overrightarrow{S_1}\cdot\overrightarrow{P} = \pm\overrightarrow{S_2}\cdot\overrightarrow{P} \end{aligned} \quad [2]$$

Where S_1 and S_2 denote the Sun at time t_1 and t_2 respectively, and $\cdot$ is the scalar product.

Moreover, if we consider a given point on the celestial sphere $\overrightarrow{P}(x_p, y_p, z_p)$, at a given time t, we have from Eq. (1):

$$\overrightarrow{S}\cdot\overrightarrow{P} = -x_p\cos\delta\sin\omega + y_p(\sin\delta\cos\phi - \cos\delta\sin\phi\cos\omega) + z_p(\cos\delta\cos\phi\cos\omega + \sin\delta\sin\phi) \quad [3]$$

DoLP is time invariant at the NCP. Having determined the condition for the DoLP to be invariant, we will now show that the DoLP is time invariant at the NCP.

At the NCP, we have: $x_p = 0$ (North bearing in ENU frame), $y_p = \cos\phi$ and $z_p = \sin\phi$ (altitude of NCP is equal to the latitude of point P). Thus, Eq. (3) becomes:

$$\begin{aligned} \overrightarrow{S}\cdot\overrightarrow{P_{NCP}} &= \cos\phi(\sin\delta\cos\phi - \cos\delta\sin\phi\cos\omega) + \sin\phi(\cos\delta\cos\phi\cos\omega + \sin\delta\sin\phi) \\ &= \cos^2\phi\sin\delta + \sin^2\phi\sin\delta = \sin\delta \end{aligned} \quad [4]$$

We notice here that the DoLP is only dependant on the Sun's declination. However, we assumed earlier that the rotation of the Earth around the Sun was negligible, meaning the declination is constant. Therefore, we can reasonably assume that the DoLP is constant at the NCP during a one day observation.

Sets of points whose DoLP is time invariant. In this section, we will seek for all the points with DoLP invariant between two successive instants t_1 and t_2. To find all the solutions, we should solve, from Eq. (2), the equations $\overrightarrow{S_1}\cdot\overrightarrow{P} = \overrightarrow{S_2}\cdot\overrightarrow{P}$ and $\overrightarrow{S_1}\cdot\overrightarrow{P} = -\overrightarrow{S_2}\cdot\overrightarrow{P}$.

First Set, radial invariance Let us consider the first equation $\overrightarrow{S_1} \cdot \overrightarrow{P} = \overrightarrow{S_2} \cdot \overrightarrow{P}$

From Eq. (3), we have :

$$\begin{aligned}\overrightarrow{S_1} \cdot \overrightarrow{P} - \overrightarrow{S_2} \cdot \overrightarrow{P} =& - x_p \cos\delta \left[\sin\omega_1 - \sin\omega_2\right] - y_p \cos\delta \sin\phi \left[\cos\omega_1 - \cos\omega_2\right] \\ &+ z_p \cos\delta \cos\phi \left[\cos\omega_1 - \cos\omega_2\right] \\ =& \cos\delta \left(-x_p \left[\sin\omega_1 - \sin\omega_2\right] + \left(-y_p \sin\phi + z_p \cos\phi\right) \left[\cos\omega_1 - \cos\omega_2\right]\right) = 0\end{aligned} \tag{5}$$

Where ω_1 and ω_2 are the hour angles related to S_1 and S_2 respectively.

Moreover, the point P can be expressed in hemispherical coordinates by two coordinates only, the azimuth α and the altitude θ (α is null for a point in the north direction and positive when turning from North to East, and θ is null for a point on the horizon and 90° at the zenith), which reduces the equation to two independent unknowns. We therefore consider $\overrightarrow{P}(\cos\theta \sin\alpha, \cos\theta \cos\alpha, \sin\theta)$. Eq. (5) then becomes:

$$\begin{aligned}\overrightarrow{S_1} \cdot \overrightarrow{P} - \overrightarrow{S_2} \cdot \overrightarrow{P} =& \cos\delta(-\cos\theta \sin\alpha \left[\sin\omega_1 - \sin\omega_2\right] \\ &+ \left(-\cos\theta \cos\alpha \sin\phi + \sin\theta \cos\phi\right) \left[\cos\omega_1 - \cos\omega_2\right]) = 0 \\ \iff \tan\theta =& \frac{\cos\alpha \sin\phi \tan\left(\frac{\omega_1+\omega_2}{2}\right) - \sin\alpha}{\cos\phi \tan\left(\frac{\omega_1+\omega_2}{2}\right)}\end{aligned} \tag{6}$$

Therefore, the set of solutions (α, θ) of the equation $\overrightarrow{S_1} \cdot \overrightarrow{P} = \overrightarrow{S_2} \cdot \overrightarrow{P}$ is:

$$\boldsymbol{Set_1} = \left\{ \left(\alpha, \tan^{-1}\left[\frac{\cos\alpha \sin\phi \tan\left(\frac{\omega_1+\omega_2}{2}\right) - \sin\alpha}{\cos\phi \tan\left(\frac{\omega_1+\omega_2}{2}\right)} \right] \right), \alpha \in [-\pi, \pi[\right\} \tag{7}$$

This set fully describes the radial invariance discussed in the article.

Check : at the NCP $\alpha = 0$, and we have a DoLP invariance between time t_1 and t_2 if $\tan\theta = \tan\phi$, that is $\theta = \phi$.

Second Set, plane invariance Let us now consider the second equation $\overrightarrow{S_1} \cdot \overrightarrow{P} = -\overrightarrow{S_2} \cdot \overrightarrow{P}$

We have from Eq. (3):

$$\begin{aligned}\overrightarrow{S_1} \cdot \overrightarrow{P} + \overrightarrow{S_2} \cdot \overrightarrow{P} =& - x_p \cos\delta \left[\sin\omega_1 + \sin\omega_2\right] + y_p(2 \sin\delta \cos\phi - \cos\delta \sin\phi \left[\cos\omega_1 + \cos\omega_2\right]) \\ &+ z_p(\cos\delta \cos\phi \left[\cos\omega_1 + \cos\omega_2\right] + 2 \sin\delta \sin\phi) = 0\end{aligned} \tag{8}$$

As before, we replace the cartesian coordinates of the point by hemispherical coordinates. We thus obtain :

$$\begin{aligned}\overrightarrow{S_1} \cdot \overrightarrow{P} + \overrightarrow{S_2} \cdot \overrightarrow{P} =& - \cos\theta \sin\alpha \cos\delta \left[\sin\omega_1 + \sin\omega_2\right] \\ &+ \cos\theta \cos\alpha(2 \sin\delta \cos\phi - \cos\delta \sin\phi \left[\cos\omega_1 + \cos\omega_2\right]) \\ &+ \sin\theta(\cos\delta \cos\phi \left[\cos\omega_1 + \cos\omega_2\right] + 2 \sin\delta \sin\phi) = 0 \\ \iff \tan\theta =& \frac{\sin\alpha \cos\delta \left[\sin\omega_1 + \sin\omega_2\right] + \cos\alpha \left(-2 \sin\delta \cos\phi + \cos\delta \sin\phi \left[\cos\omega_1 + \cos\omega_2\right]\right)}{\cos\delta \cos\phi \left[\cos\omega_1 + \cos\omega_2\right] + 2 \sin\delta \sin\phi}\end{aligned} \tag{9}$$

Finally, the set of solutions (α, θ) of the equation $\overrightarrow{S_1} \cdot \overrightarrow{P} = -\overrightarrow{S_2} \cdot \overrightarrow{P}$ is:

$$\boldsymbol{Set_2} = \left\{ \left(\alpha, \tan^{-1}\left[\frac{\sin\alpha \cos\delta \left[\sin\omega_1 + \sin\omega_2\right] + \cos\alpha \left(-2 \sin\delta \cos\phi + \cos\delta \sin\phi \left[\cos\omega_1 + \cos\omega_2\right]\right)}{\cos\delta \cos\phi \left[\cos\omega_1 + \cos\omega_2\right] + 2 \sin\delta \sin\phi} \right] \right), \alpha \in [-\pi, \pi] \right\} \tag{10}$$

This set fully describes the plane invariance discussed in the article.

Remark : for an observer located on earth, the only visible solutions are those with $\theta \geq 0$ (without considering earth curvature effects).

The NCP is the only point included in the radial invariance set at any time. This part aims at showing that if a point is on the radial invariance for different times, then this point is necessarily the NCP.

Let $(\omega_1, \omega_2) \in [-\pi, \pi[^2$, and $\boldsymbol{Set_1}_{(\omega_1,\omega_2)}$ the set of $(\alpha, \theta) \in [-\pi, \pi[^2$ solution of $\overrightarrow{S_{\omega_1}} \cdot \overrightarrow{P(\alpha, \theta)} = \overrightarrow{S_{\omega_2}} \cdot \overrightarrow{P(\alpha, \theta)}$, with $\overrightarrow{S_{\omega_1}}$ and $\overrightarrow{S_{\omega_2}}$ the sun vectors at time ω_1 and ω_2 respectively. Let us show the assertion : $\forall(\omega_1, \omega_2) \in [-\pi, \pi[^2, (\alpha, \theta) \in \boldsymbol{Set_1}_{(\omega_1,\omega_2)} \iff (\alpha, \theta) = (0, \phi)$.

Demonstration We already know that $(0,\phi)$ is always in $\boldsymbol{Set_1}_{(\omega_1,\omega_2)}$. Let us show that this solution is unique. Let $(\omega_1,\omega_2,\omega_3) \in [-\pi,\pi[^2$, and $(\alpha,\theta) \in \boldsymbol{Set_1}_{(\omega_1,\omega_2)} \cap \boldsymbol{Set_1}_{(\omega_1,\omega_3)}$.

Since $(\alpha,\theta) \in \boldsymbol{Set_1}_{(\omega_1,\omega_2)}$, we have:

$$\tan\theta = \frac{\cos\alpha \sin\phi \tan\left(\frac{\omega_1+\omega_2}{2}\right) - \sin\alpha}{\cos\phi \tan\left(\frac{\omega_1+\omega_2}{2}\right)} \tag{11}$$

We also have $(\alpha,\theta) \in \boldsymbol{Set_1}_{(\omega_1,\omega_3)}$, so :

$$\tan\theta = \frac{\cos\alpha \sin\phi \tan\left(\frac{\omega_1+\omega_3}{2}\right) - \sin\alpha}{\cos\phi \tan\left(\frac{\omega_1+\omega_3}{2}\right)} \tag{12}$$

Without loss of generality, we set $t_1 = \frac{\omega_1+\omega_2}{2}$ and $t_2 = \frac{\omega_1+\omega_3}{2}$. Then, from Eq. (11) and Eq. (12), and since $\theta \in [-\pi,\pi[$, we have

$$\frac{\cos\alpha \sin\phi \tan t_1 - \sin\alpha}{\cos\phi \tan t_1} = \frac{\cos\alpha \sin\phi \tan t_2 - \sin\alpha}{\cos\phi \tan t_2} \tag{13}$$

By assuming $t_1, t_2 \neq 0$ and $\phi \neq \pm\frac{\pi}{2}$, we have from Eq. (13):

$$\sin\alpha \cos\phi \tan t_2 = \sin\alpha \cos\phi \tan t_1 \tag{14}$$

Therefore, since $\phi \neq \pm\frac{\pi}{2}$ and assuming $t_1 \neq t_2$, we must have $\sin\alpha = 0$. Thus $\alpha \in \{0,-\pi\}$. If $\alpha = 0$, then $\theta = \phi$, and if $\alpha = -\pi$, then $\theta = -\phi$. Yet, for an observer located on the earth surface only positive altitudes are considered, so $(\alpha,\theta) = (0,\phi)$ (observer on North hemisphere), which is by definition the NCP position.

There is no point included in the plane invariance set at any time. In this section, we will show that their is no point such as the NCP in the plane invariance set.

Let us consider $(\omega_1,\omega_2) \in [-\pi,\pi[^2$, and $\boldsymbol{Set_2}_{(\omega_1,\omega_2)}$ the set of $(\alpha,\theta) \in [-\pi,\pi[^2$ solution of $\overrightarrow{S_{\omega_1}} \cdot \overrightarrow{P(\alpha,\theta)} = -\overrightarrow{S_{\omega_2}} \cdot \overrightarrow{P(\alpha,\theta)}$

Let us show the assertion :

$$\exists(\phi,\delta) \in [-\frac{\pi}{2},\frac{\pi}{2}] \times [-0.41,0.41], \forall(\alpha,\theta) \in [-\pi,\pi[^2, \exists(\omega_1,\omega_2) \in [-\pi,\pi[^2, (\alpha,\theta) \notin \boldsymbol{Set_2}_{(\omega_1,\omega_2)} \tag{15}$$

We know from Eq. (10) that for a given $(\omega_1,\omega_2,\omega_3) \in [-\pi,\pi[^3$,

$$\begin{aligned} &(\alpha,\theta) \in \boldsymbol{Set_2}_{(\omega_1,\omega_2)} \\ &\iff \tan\theta = \frac{\sin\alpha\cos\delta\left[\sin\omega_1+\sin\omega_2\right] + \cos\alpha\left(-2\sin\delta\cos\phi + \cos\delta\sin\phi\left[\cos\omega_1+\cos\omega_2\right]\right)}{\cos\delta\cos\phi\left[\cos\omega_1+\cos\omega_2\right] + 2\sin\delta\sin\phi} \end{aligned} \tag{16}$$

and

$$\begin{aligned} &(\alpha,\theta) \in \boldsymbol{Set_2}_{(\omega_1,\omega_3)} \\ &\iff \tan\theta = \frac{\sin\alpha\cos\delta\left[\sin\omega_1+\sin\omega_3\right] + \cos\alpha\left(-2\sin\delta\cos\phi + \cos\delta\sin\phi\left[\cos\omega_1+\cos\omega_3\right]\right)}{\cos\delta\cos\phi\left[\cos\omega_1+\cos\omega_3\right] + 2\sin\delta\sin\phi} \end{aligned} \tag{17}$$

Therefore, from Eq. (16) and Eq. (17), and since $\theta \in [-\pi,\pi[$,

$$\begin{aligned} &(\alpha,\theta) \in \boldsymbol{Set_2}_{(\omega_1,\omega_2)} \cap \boldsymbol{Set_2}_{(\omega_1,\omega_3)} \\ \iff &\frac{\sin\alpha\cos\delta\left[\sin\omega_1+\sin\omega_2\right] + \cos\alpha\left(-2\sin\delta\cos\phi + \cos\delta\sin\phi\left[\cos\omega_1+\cos\omega_2\right]\right)}{\cos\delta\cos\phi\left[\cos\omega_1+\cos\omega_2\right] + 2\sin\delta\sin\phi} \\ &- \frac{\sin\alpha\cos\delta\left[\sin\omega_1+\sin\omega_3\right] + \cos\alpha\left(-2\sin\delta\cos\phi + \cos\delta\sin\phi\left[\cos\omega_1+\cos\omega_3\right]\right)}{\cos\delta\cos\phi\left[\cos\omega_1+\cos\omega_3\right] + 2\sin\delta\sin\phi} = 0 \end{aligned} \tag{18}$$

Let us consider $f : [-\pi,\pi[\to \mathbb{R}$ such that

$$\begin{aligned} f(\alpha) = &\frac{\sin\alpha\cos\delta\left[\sin\omega_1+\sin\omega_2\right] + \cos\alpha\left(-2\sin\delta\cos\phi + \cos\delta\sin\phi\left[\cos\omega_1+\cos\omega_2\right]\right)}{\cos\delta\cos\phi\left[\cos\omega_1+\cos\omega_2\right] + 2\sin\delta\sin\phi} \\ &- \frac{\sin\alpha\cos\delta\left[\sin\omega_1+\sin\omega_3\right] + \cos\alpha\left(-2\sin\delta\cos\phi + \cos\delta\sin\phi\left[\cos\omega_1+\cos\omega_3\right]\right)}{\cos\delta\cos\phi\left[\cos\omega_1+\cos\omega_3\right] + 2\sin\delta\sin\phi} \end{aligned} \tag{19}$$

Let us consider some fixed parameters, for example $\delta = 0.2$, $\phi = \frac{\pi}{4}$, $\omega_1 = 0$, $\omega_2 = \frac{\pi}{5}$. By plotting this function for $\alpha \in [-\pi,\pi[$, and $\omega_3 \in \left\{\frac{2\pi}{5}; \frac{3\pi}{5}\right\}$, we see that when $\omega_3 = \frac{2\pi}{5}$, α solutions of $f(\alpha) = 0$ are not solution of $f(\alpha) = 0$ when $\omega_3 = \frac{3\pi}{5}$. Therefore there is no $(\alpha,\theta) \in [-\pi,\pi[^2$ such that $(\alpha,\theta) \in \boldsymbol{Set_2}_{(0,\frac{\pi}{5})} \cap \boldsymbol{Set_2}_{(0,\frac{2\pi}{5})} \cap \boldsymbol{Set_2}_{(0,\frac{3\pi}{5})}$.

Measurement device

Experimental data were obtained with a division of focal plane color-polarimetric camera (PHX050S-QC from Lucid Vision Labs, sensor ref. Sony IMX250MYR) topped with a 185° fisheye lens (Fujinon FE185C57HA-1). The camera was installed on the roof of the INT Lab at La Timone, Marseille, France (43.286990365824785°N, 5.403361407820939°E), and was roughly pointing towards the zenith. Data were acquired on 23 September 2022 with an aperture of $f/2.8$. As the device was left several days unmoved on the roof, an orientation calibration was performed. In order to make the Sun appear as a spot on the sensor, several clear sky pictures were taken with minimal time of exposure ($34\mu s$). Then, the successive positions of the Sun were computed each time as the centroïd of the spot on the sensor plane. Next, with the distortion model provided by the manufacturer, we transformed the 2D centroïds coordinates to 3D hemispherical coordinates in the camera frame. We also used the Matlab calibration camera toolbox to estimate the intrinsic parameters (focal length and center of distorsion in pixels) of the camera with a fisheye lens. Simultaneously, we computed the groundtruth positions of the Sun in the ENU frame centered on the camera by using ephemeris estimated with the AstroPy python library (4). We therefore had two sets of solar vectors, a set of groundtruth solar vectors expressed in the ENU frame and a set of measured solar vectors expressed in the camera frame. The optimal rotation between the two sets of vectors derived in the least-squares (5) way allowed us to deduce the rotation matrix between the two frames and finally the absolute camera orientation. The Degree of Linear Polarization (DoLP) was calculated by selecting only the blue channel and by making the assumption that the four micro-polarizers of a pixel cluster (6) was roughly viewing the same spot in the sky.

Our data were first preprocessed with a circular averaging filter. Next, we implemented the absolute difference in DoLP between several moments of time. The NCP was located by searching for the maximum valued point, namely the intersection between all the radial invariance axes (cf. figure 1d). Lastly, the coordinates of the point were transformed to North and latitude coordinates and compared with the ground truth values.

Data availability

All the data used for camera calibration, from further outdoor experiments with a polarimetric camera placed on the rooftop of a laboratory in Marseille and from further simulation experiments are available with their related programs (Matlab and Python) on the following OSF link: https://osf.io/fcsgk/?view_only=01d95ac195a14b65a113fb6a9381f25a

References

1. WM Smart, *Textbook on Spherical Astronomy* ed. RM Green. (Cambridge University Press), 6 edition, (1977).
2. B Suhai, G Horvath, How well does the rayleigh model describe the e-vector distribution of skylight in clear and cloudy conditions? a full-sky polarimetric study. *J. Opt. Soc. Am. A, Opt. image science, vision* **21**, 1669–76 (2004).
3. A Sproul, Derivation of the solar geometric relationships using vector analysis. *Renew. Energy* **32**, 1187–1205 (2007).
4. Astropy Collaboration, et al., The Astropy Project: Sustaining and Growing a Community-oriented Open-source Project and the Latest Major Release (v5.0) of the Core Package. *apj* **935**, 167 (2022).
5. M Newville, T Stensitzki, DB Allen, A Ingargiola, LMFIT: Non-Linear Least-Square Minimization and Curve-Fitting for Python (2014).
6. F Freitas Carvalho, C Augusto de Moraes Cruz, G Costa Marques, K Martins Cruz Damasceno, Angular light, polarization and stokes parameters information in a hybrid image sensor with division of focal plane. *Sensors* **20** (2020).

List of Abbreviations and Symbols

α_P azimuth angle of a point P

θ_P altitude/elevation angle of a point P

ϕ observer's latitude

δ sun declination

ω sun hour angle

γ_P scattering angle of a point P with respect to the Sun's position

x_p East coordinate of a point P in the ENU frame

y_p North coordinate of a point P in the ENU frame

z_p Up/Zenith coordinate of a point P in the ENU frame

$\overrightarrow{P}$ unit vector going from the origin of the ENU frame O to a point P on the celestial sphere

ENU East North Up frame

DoLP Degree of linear polarization

NCP North celestial pole